Performance of polymeric membranes treating ozonated surface water: Effect of ozone dosage

Accepted for publication in Separation and Purification Technology

on September 27, 2010

Published article DOI: 10.1016/j.seppur.2011.07.021

Seokjong Byun, Julian S. Taurozzi, Alla L. Alpatova, Fulin Wang, Volodymyr V. Tarabara*

Department of Civil and Environmental Engineering, Michigan State University, East Lansing, MI 48824, USA

* Corresponding author: email: tarabara@msu.edu; fax: +1 (517) 355-0250

Abstract

Ozonation may have a significant impact on downstream water treatment unit processes. In this study, the effect of pre-ozonation of the feed surface water on the flux and rejection performance of polymeric nanofiltration (NF) and ultrafiltration (UF) membranes was investigated. The fouling and dissolved organic carbon (DOC) rejection characteristics of the membranes were found to depend on the ozonation dosage. In UF experiments, the DOC rejection was relatively low (11 % to 26 %) and was found to increase slightly with an increase in the ozone dosage. The increase in rejection with the ozone dosage was interpreted to stem from the higher polarity of ozonated NOM constituting the DOC-rejecting fouling layer. The propensity of the feed water to foul UF membranes increased with ozone dosage but the increase was statistically significant only at 82% confidence interval. In NF experiments, the increase in ozone dosage led to a statistically significant increase in the permeate flux while rejection remained consistently above 92 %. The combined pore blockage-cake filtration model was applied to interpret NF flux data in terms of the dominant fouling mechanisms. Pore blockage, cake filtration and a transition regime were identified. Although pre-ozonation led to the formation of NF membrane cakes with higher specific resistance, the overall added hydraulic resistance due to fouling was lowered apparently due to a decrease in cake thickness.

Key Words: membrane fouling, ozonation, fouling mechanisms, nanofiltration, ultrafiltration.

1. Introduction

Our increasing demand for potable water has broadened the range of water sources considered for treatment and has spurred research into water purification technologies capable of treating lower quality waters in a cost-efficient manner. Membrane filtration is an example of a technology that can treat source waters of a wide range of compositions to produce a high quality effluent. Nanofiltration (NF) membranes can remove natural organic matter (NOM) prior to the application of disinfectants; as a result, trihalomethane formation potential can be reduced significantly [1-3]. Combining membrane separation with disinfection processes [4-6] such as ozonation (e.g., [7, 8]) implements a multiple barrier treatment approach that can ensure that stringent disinfection standards are met without exceeding the maximum allowable concentration of trihalomethanes in the product water. Examples of treatment facilities where membrane separation is combined with ozonation to treat surface water include the world's largest NF and ultrafiltration (UF) plants located in Méry-sur-Oise (France) and Mississauga (Ontario, Canada), respectively. The NF treatment line at the Méry-sur-Oise plant was added specifically to improve the removal of dissolved organic matter [9, 10]. The UF membrane filtration unit at the plant in Mississauga is combined with ozonation and biologically activated carbon contactors to meet water quality regulations and improve the water's aesthetic quality (i.e., taste, odor and color).

Because of the typically high NOM content and the resultant high fouling potential of surface waters, pretreatment is required prior to nanofiltration. However, even pretreated water contains impurities that can impair the performance of downstream membrane processes [11-14]. The nature of residual contaminants depends, in part, on the choice of pretreatment. Oxidation pretreatment processes are applied for primary disinfection and microbial growth control. Such preliminary oxidation (e.g., pre-chlorination and pre-

ozonation) may alter the chemical nature of contaminants that can persist in the treatment train. The transformation of NOM during pre-chlorination or pre-ozonation is an example of such changes. Studies that included autopsies of NF membranes from the Méry-sur-Oise plant revealed that most of the fouling layer on the membrane surface consisted of organic material [15-17]; given that the treatment train in the plant included ozonation as one of steps preceding membrane filtration, the membrane foulants were ozonated organic material, including ozonated NOM.

The physicochemical properties of ozonated NOM can differ significantly from those of parent NOM molecules [18-20]. During the ozonation of NOM-containing waters, molecular ozone and hydroxyl radicals (·OH) oxidize NOM molecules and change their hydrophilicity and polarity thus affecting their propensity to foul membranes [18-21]. Ozonation can also result in changes in the molecular weight of aqueous NOM. Even small ozone dosages (< 1.0 mg of gaseous O_3 per mg of dissolved organic matter) can turn large hydrophobic NOM molecules into intermediate or low molecular weight molecules and increase their oxygen content [18, 22, 23]. Higher ozone dosages can lead to a significant decomposition of large molecular weight NOM molecules [24] and can eventually result in the complete oxidation (i.e., mineralization) of NOM [25].

While membrane fouling by NOM has been studied extensively (e.g., [26, 27]), little is known about the fouling properties of oxidized NOM. Most studies published to date on the subject report data on the performance of membrane filtration plants [13-15, 17] without exploring the fundamental underlying causes for the observed oxidation-induced changes in membrane fouling due to pre-oxidation. The present study aims at addressing this knowledge gap. The specific objective of this work was to identify the effects of pre-ozonation with low ozone dosages (often applied for color and odor removal [28]) on the flux and rejection behavior of UF and NF membranes treating surface waters.

2. Materials and Methods

2.1 Feed water

Water samples were taken from Lake Lansing, a borderline eutrophic lake. Samples were collected at the boat ramp at the Lake Lansing Park – South, Haslett, MI in five-gallon carboys and stored at 4 ^{o}C in a refrigerator. Water samples were pre-filtered through a 0.5-μm ceramic cartridge microfilter (Doulton USA, Southfield, MI). The water quality parameters are summarized in Table 1. The total dissolved organic carbon (DOC) of the water was 11.7 ± 0.1 mg(DOC)/L. Other water quality parameters for Lake Lansing water have been reported elsewhere [8, 29].

[Table 1]

2.2 Ozonation apparatus

Ozone was generated by passing oxygen gas through an ozone generator (Ozotech Inc., OZ2PCS-V, USA) creating a (4 to 9) kV corona discharge and producing ozone at a rate of (0.26 to 0.6) g/h (Fig. 1). Oxygen from an oxygen gas cylinder passed through a dehumidification column and entered a gas flow controller, where the gas flow rate was set and kept constant at 1.0 L/min during the experiments. Inlet gas-phase ozone concentrations were established by varying the voltage of the input coil of the boosting transformer, a component of the ozone generator. By using a needle valve, the ozone-oxygen mixture was directed to a 500 mL ozonation batch reactor equipped with a porous plate for the dispersion of gas bubbles. The inlet and outlet gas lines were connected to a

quartz cell in a UV-vis spectrophotometer (Spectronic Genesys 5, Milton Roy, Inc.) to determine the gas phase ozone concentrations by measuring UV absorption at 254 nm wavelength. The molar extinction coefficient for ozone (ε_{254} = 3,000 $M^{-1}\cdot cm^{-1}$) was used to calculate the inlet and outlet concentrations of gaseous ozone based on the measured UV absorption data. Residual ozone in the gas flow was captured and decomposed in a potassium chloride trap installed downstream from the batch reactor.

[Figure 1]

The aqueous ozone dosage was calculated based on the total amount of transferred ozone as follows. First, the ozone mass transfer rate, $k_L a_{O_3}$, was measured in an ozone transfer experiment with ultrapure distilled water at pH 2 ($[O_3]_g$= 1 mg/L, T = (20±0.5) ^oC; gas flow rate = 1 L/min) in the absence of molecular ozone sinks (e.g., $OH^\bullet$, organics). The feed water was produced by a commercial ultrapure water system (Lab Five, USFilter Corp., Hazel Park, MI) equipped with a terminal 0.2 µm capsule microfilter (PolyCap, Whatman Plc., Sanford, ME) and had a conductivity of 0.06 µS/cm. An ozone transfer rate $k_L a_{O_3}$ of 0.019 s^{-1} was calculated from the following expression:

$$k_L a_{O_3} = \frac{1}{t}\ln\left(\frac{C^* - C_0}{C^* - C_t}\right), \quad (1)$$

where C^* is the aqueous concentration of ozone in equilibrium with the gaseous ozone [30], C_0 is the initial aqueous concentration of ozone, and C_t is the aqueous concentration at time t. Then, the total transferred ozone, in mg(O_3)/L, was calculated as follows:

$$C = \int_0^t k_L a_{O_3} \left(C^* - C_t\right) dt \quad (2)$$

Finally, the ozone utilization rate of the system was determined to be 31%, by dividing the total transferred ozone by the total applied gaseous ozone.

2.2.1 Ozonation procedure

A 500 mL sample was ozonated at $C_{O_3(gas)}$ = 1.0 mg/L, gas flow rate of 1 L/min and temperature of (20 ± 0.5) °C. The aqueous ozone dosages were zero (i.e., no pre-ozonation), 0.23 and 0.93 mg(O_3)/mg(DOC); these dosage values corresponded to reaction times of 0 min, 5 min, and 16 min and were typical dosages that are used at water treatment plants to reduce color and odor in surface waters [28]. Since the skin of NF90 membrane is composed of aromatic polyamide, which can be easily degraded by ozone, it was important to ensure the absence of ozone in the feed water when in contact with the membranes; to remove the residual ozone from the water samples, they were sealed and vigorously mixed for 1 h immediately after ozonation. The indigo method [31] was used to measure the residual ozone and ascertain its removal to levels below the detection limit (0.005 mg/L) of the method.

2.3 Membranes

Two commercially available polymeric membranes were used in this study: a UF polyvinylidene fluoride (PVDF) membrane with a molecular weight cutoff (MWCO) of 30 kDa and an NF aromatic polyamide membrane, NF90 (FilmTec), with a MWCO in the 200 Da to 400 Da range (Table 2). Each membrane coupon was soaked overnight in ultrapure water.

Prior to each experiment, membrane coupons were compacted by filtering ultrapure water at a transmembrane pressure of 40 psi (0.276 MPa) for UF membranes, or 140 psi (0.965 MPa) for NF membranes until a steady-state permeate flux was achieved.

[Table 2]

2.4 Membrane filtration experiments

Filtration experiments were performed using a normal flow (i.e., dead-end) membrane filtration cell (HP 4750, Sterlitech Corp.; membrane area of 14.6 cm^2). Filtration tests conducted to generate flux data for blocking law analysis (see section 3.2.1) were performed in unstirred conditions; all other filtrations were performed with stirring at a constant rate of approximately 300 rpm to simulate crossflow conditions. In each experiment, 200 mL of ozonated Lake Lansing water were filtered at a temperature of (20 ± 0.5) ^oC. The transmembrane pressure was maintained at 40 psi (0.276 MPa) in UF tests and at 140 psi (0.965 MPa) in NF tests by connecting the filtration cell to a pressured nitrogen gas tank. In the ultrafiltration experiments, we observed a significant membrane-to-membrane variability in the hydraulic resistance of unfouled membranes. For this reason, two sets of triplicate experiments were performed, covering a wide range (74 to 173 $L/m^2 \cdot h$) of initial fluxes. Permeate samples were collected and measured for DOC to determine the DOC rejection by the membranes. For each experiment, two permeate samples were collected, one at the beginning of the fouling experiment (first 40 mL of permeate) and one at the end (40 mL of permeate obtained after 120 mL of feed had been filtered). The permeate was collected on a mass balance (OHAUS Corp. USA) and the data were automatically logged into a computer (Fig. 1). All experiments were performed in triplicates.

2.5 DOC fractionation

Five Amicon cellulose acetate membranes (YC05, YM1, YM3, YM10, YM30) with apparent MWCO values of 0.5, 1.0, 3.0, 10.0 and 30.0 kDa, correspondingly, were used to fractionate DOC in the raw and ozonated feed water by adapting the procedure described by Mellema [32]. Prior to filtration tests, the YC05 membranes were soaked in 1M NaCl for 30 min, while the membranes of the YM series were soaked in 0.1 M NaOH for 30 min; after this, 100 ml of ultrapure water were filtered through each membrane. Finally, five 200 ml Lake Lansing water samples were filtered in parallel using five stirred Amicon 8200 ultrafiltration cells. The transmembrane pressure was maintained at 55 psi (0.379 MPa).

2.6 Analytical methods

The ozonation-induced changes in the molecular structure and chemistry of feed water organics were characterized by measuring $UV_{254,}$ Abs_{436} (used to quantify the degree of color removal [33]), DOC, and zeta potential of the colloids in the feed water. Based on measured UV_{254} and DOC values, the specific UV_{254} absorbance ($SUVA_{254}$) was calculated as UV_{254}/DOC. UV-vis absorption measurements were performed using a UV-vis spectrophotometer (Spectronic Genesys 5, Milton Roy, Inc.). DOC was measured using a Total Organic Carbon analyzer (1010, O I Analytical, USA) equipped with a 1051 Vial Autosampler. The zeta potential was calculated using the Smoluchowski model based on the electrophoretic mobility measured at (24.5 ±0.5) °C (ZetaPALS, Brookhaven Instrument Corp., Holtsville, NY). Measurements of zeta potential were performed within 2 h after ozonation of the water samples. Streaming potential of the membranes was measured using an Anton Paar Electrokinetic Analyzer. Membranes were soaked in water prior to the measurements, which were conducted in 10 mM KCl.

Contact angles were measured using an FTÅ 200 analyzer (First Ten Ångstroms, Portsmouth, VA) following the procedure described previously [34].

2.7. Application of pore blocking analysis

Blocking filtration laws, first proposed by Hermans and Bredée [35] and subsequently developed by Gonsalves [36], describe four mechanisms of membrane fouling: complete pore blocking (also called pore sealing), standard pore blocking (also called pore constriction), intermediate pore blocking, and cake filtration. The first three mechanisms are categorized as pore blocking. Hermia [37] demonstrated that, for membrane filtration carried out in a constant transmembrane pressure mode with the feed flow normal to the membrane surface and with foulants of spherical shape that are completely retained, a common characteristic equation for different fouling mechanisms can be derived:

$$\frac{d^2t}{dV^2} = k\left(\frac{dt}{dV}\right)^n, \tag{3}$$

where k is a constant and n is the blocking index equal to 2, 1.5, 1, or 0 for complete blocking, standard blocking, intermediate blocking, and cake filtration, respectively. Equation (3) is typically used to identify blocking mechanisms by determining the value of the blocking index n in the plot of $\frac{d^2t}{dV^2}$ against $\frac{dt}{dV}$ [38-44]. In several studies, the value of n for later stages of filtration was reported to be negative [38-42] pointing to the failure of blocking laws to explain the flux data.

The combined pore blockage-cake filtration model proposed by Ho and Zydney [44] describes simultaneous pore blockage and formation of the cake over blocked areas of the membrane. The negative slope of the $\frac{d^2t}{dV^2}\left(\frac{dt}{dV}\right)$ dependence finds its explanation in the

model as corresponding to the transition from pore blockage to cake filtration regime. According to the model, the transient permeate flux, $J(t)$, is given by:

$$\frac{J(t)}{J_0} = F_1(t) + \frac{R_m}{R_{c0}} \frac{1 - F_1(t)}{F_2(t)}, \quad (4)$$

where $F_1(t) = \exp\left(-\frac{\alpha \Delta P C_{DOC}}{\mu R_m} t \right)$ and $F_2(t) = \sqrt{1 + \frac{2 f' R' \Delta P C_{DOC}}{\mu (R_m + R_{c0})^2} t}$. The first term in eq. (4) corresponds to the flow through open pores while the second term describes the flow through blocked pores. In this equation, J_0 (m/s) is the initial flux (the flux from the unfouled membrane); R_m (m^{-1}) is the hydraulic resistance of the unfouled membrane; C_{DOC} (kg/m^3) is the DOC concentration in the bulk of the feed solution; R_{c0} (m^{-1}) is the initial resistance of the membrane cake; f' is the DOC fraction that contributes to cake growth; R' (m/kg) is the specific resistance of the membrane cake; and α (m^2/kg) is the pore blockage parameter. J_0, R_m, and C_{DOC} are measurable experimental variables while $f'R'$, R_{c0}, and α can used as fitting parameters to match experimental and modeled $J(t)$.

Yuan et al. have successfully applied the model to describe flux decline during stirred cell microfiltration of aqueous solutions of Aldrich humic acid [40] through 0.2 μm track etched membranes. A very good fit between the model and the experimental flux data was observed over most but not all of the duration of the experiment. The discrepancies observed during later stages of filtration were attributed to the enhanced back-transport of the foulants.

3. Results and Discussion

3.1. Characteristics of ozonated Lake Lansing water

Physicochemical parameters of the feed water before and after ozonation are summarized in Table 1. Upon ozonation, pH increased from 8.0 to 8.3 while DOC concentration slightly decreased from 11.7 mg/L to 10.9 mg/L. These changes were accompanied by a noticeable attenuation of color that corresponded to a decrease in absorption at the 436 nm wavelength. Ozonation led to a decrease of the SUVA value from 2.01 $L \cdot mg^{-1} \cdot cm^{-1}$ to 1.03 $L \cdot mg^{-1} \cdot cm^{-1}$ with most of this decrease observed already after the application of the (lowest) 0.23 $mg(O_3)/mg(DOC)$ dosage. This change was indicative of the decreased aromaticity of NOM in the solution [45]. The ozonation-induced changes in the apparent molecular weight of NOM were not statistically significant ($p > 0.05$) at the 95 % confidence interval (Fig. 2), which can be attributed to high concentration of alkalinity (~ 150 mg/L as $CaCO_3$) in Lake Lansing and resulting scavenging of OH radicals by carbonate species. This implies that the ozone dosage was not sufficiently high for a significant decrease in apparent molecular weight to be observed.

[Figure 2]

3.2. Membrane fouling propensity of ozonated feed water

Previous studies on the fouling of UF [46, 47] and NF [13] membranes by ozonated NOM suggest that the effect of ozonation on fouling is complex and dependent on water composition and ozone dosage. Hyung et al. showed that ozonation brought about a decrease in reversible fouling resistance and an increase in irreversible fouling of UF

membranes [46]. In experiments with NF membranes, Lee et al. reported that ozonation did not cause a significant reduction in fouling [14]. In experiments with natural waters pretreated by coagulation and sand filtration, Kim et al. (2007) showed that ozonation followed by biological activated carbon adsorption did not lead to a decrease in the membrane fouling index [13].

In our study, the total resistance added due to fouling, R_f, was determined at the end of each filtration experiment as:

$$R_f = \left(J_0 J^{-1} - 1\right) R_m . \quad (6)$$

The changes in the fouling propensity of ozonated water can be partially attributed to the decrease in feed DOC due to ozone-induced mineralization. To factor out the effect of partial mineralization of DOC on the fouling propensity, the absolute value of the measured total fouling resistance R_f was normalized by the DOC concentration in the feed. By comparing R_f/DOC values recorded in different experiments, the fouling propensity of the feed water as a function of ozonation dosage and membrane type (UF, NF) was evaluated.

In ultrafiltration experiments, the values of the transient permeate flux were higher for water ozonated at the 0.93 mg(O_3)/mg(DOC) dosage in comparison with the flux for non-ozonated water (Fig 3a). After accounting for the slight ozonation-induced decrease in feed DOC (Table 1), a trend of increasing R_f/DOC with increasing ozone dosage remained (Fig. 3b) but the increase was not statistically significant for the 95% confidence interval. Only when the confidence interval was decreased to 82% did the differences between R_f/DOC values in UF experiments with feed water ozonated at different ozone dosages become

statistically significant. A similar behavior had been observed in previous studies with UF membranes where inconsistent changes in irreversible fouling resistance as a function of ozone dosage were reported [46, 47].

[Figure 3]

In NF experiments, pre-ozonation was observed to lead to an increase in the transient permeate flux (Fig 3b). R_f /DOC values decreased significantly (p < 0.05; 95 % confidence interval) as the ozone dosage increased (Fig. 3d), indicating that pre-ozonation even at low applied ozone dosages decreases the propensity of the feed water to foul NF membranes.

3.2.1 Application of combined pore-blockage-cake filtration model

The analysis of pore blocking laws applied to non-stirred filtration flux data was inconclusive and could not unequivocally attribute specific fouling mechanisms to a specific combination of pre-ozonation dosage and membrane type (data not shown). This was most likely because several fouling mechanisms were operative at the same time. To gain an insight into the relative importance and parameters of the fouling mechanisms we applied the combined pore blockage-cake filtration model to the same data set. The results of the fit are shown in Fig. 4.

Nanofiltration data plotted in the $\frac{d^2t}{dV^2}\left(\frac{dt}{dV}\right)$ format (Fig. 4a) included three segments that corresponded to pore blockage (n =2), cake filtration (n =0), and the transition between these two regimes (n <0) (Figure 4a). The values of experimental variables (J_0, R_m, and

C_b) and fitting parameters ($f'R'$, R_{c0}, and α) are given in Table 3. Corresponding values reported by Yuan et al. [40] are given for comparison.

[Table 3]

The pore blockage parameter, α, describes membrane area blocked per unit mass of the foulant deposited. It follows that α^{-1} (kg/m^2) has the physical meaning of the amount of organic carbon that contributes to pore blocking per unit area of the membrane. Comparison of the total amounts of organic carbon detained by NF membranes in our experiments ($C_b V_{tot} R$) with corresponding α^{-1} values indicates that only a very small fraction of filtered solids blocks pores. For example, the value of α determined by the fitting of flux data from the experiment on nanofiltration of non-ozonated feed water is 9,200 m^2/kg, which corresponds to α^{-1} of $1.09 \cdot 10^{-4}$ kg/m^2. In the related experiment, 79.54 mL of 11.7 mg(DOC)/L were filtered through the $1.46 \cdot 10^{-3}$ m^2 of NF membrane area. Assuming no back transport of DOC away from the membrane surface and taking into account the 97.65% rejection, the α value of 162 m^2/kg is obtained, which corresponds to α^{-1} of $6.17 \cdot 10^{-3}$ kg/m^2. The discrepancy between $\alpha^{-1} = 1.09 \cdot 10^{-4}$ kg/m^2 obtained by fitting experimental data and $\alpha^{-1} = 6.17 \cdot 10^{-3}$ kg/m^2 (expected based on experimentally determined values of feed concentration, filtered volume, and rejection) indicates that only a small fraction (less than 2% in this test) of organic carbon detained by the membrane contributes to pore blocking with the rest of the carbon being back-transported into the bulk of the solution and away from the membrane or incorporated into the membrane cake.

The values of α determined for the NF90 membrane are 3 to 4 orders of magnitude higher that α values reported by Yuan et al [40] for humic acid fouling a 0.2 μm track etched

membrane. This difference implies that a much smaller amount of organic carbon is sufficient to block the pores of NF membranes, which is likely due to both the smaller number of pores that can be blocked and the smaller volume of such pores. The values of α in experiments with ozonated feed water were even higher. Given that the molecular weight distribution of DOC did not significantly change upon ozonation, this trend in α can be attributed to the lesser propensity of more hydrophilic DOC to enter and block same NF pores due to higher hydrophilic repulsion [34].

The cake growth parameter, $f'R'$, has the physical meaning of the specific cake resistance (R') corrected for the fraction of DOC that contributes to cake growth. R_{c0} has the physical meaning of the initial resistance of the deposit, i.e. the hydraulic resistance of a monolayer of foulant molecules on the membrane surface. The analysis of how R_{c0}, and $f' \cdot R'$ change as a function of the ozone dosage reveals that pre-ozonation results in a membrane deposit which is highly permeable initially (low R_{c0}) but then grows into a cake with a higher specific hydraulic resistance (high $f' \cdot R'$) than that of a membrane cake formed from non-ozonated organics. Given that the total added hydraulic resistance ($R_f \cdot (C_{DOC})^{-1}$, see eq. (7)), due to fouling is lower in NF experiments with ozonated waters (Fig. 3c, Fig. 3d), eq. (7) indicates that the thickness of the cake, δ, should be smaller when the organics that form the cake were ozonated.

$$\frac{R_f}{C_{DOC}} = \delta \cdot f'R' \tag{7}$$

In our previous study, we filtered ozonated and non-ozonated aqueous solutions of Suwannee River natural organic matter through 1 kDa polyethersulfone membranes and showed that thinner fouling layers form when the feed solution is ozonated [34]. Thus, it

appears that ozonation of the membrane feed results in the formation of thinner cakes with higher specific resistance but smaller total hydraulic resistance.

In contrast to NF data, all three sets of UF data (Fig. 4b) had negative slopes. Noting that the only portion of the pore blockage-cake filtration model curve that has a negative slope corresponds to the transition between pore blockage (positive slope) and cake filtration (zero slope) we conclude that throughout UF filtration tests reported here the transition regime was operative. As such the UF dataset was too limited to be fit meaningfully by the combined pore blockage-cake filtration model.

3.3. DOC rejection by UF and NF membranes

To determine the DOC rejection by UF and NF membranes, DOC concentration in the permeate was measured at the beginning and at the end of each filtration experiment. Based on these measurements, the values of initial and final observed rejection R_{obs} were calculated (Fig. 5).

[Figure 5]

In UF experiments, ozonation led to an increase in DOC rejection. This trend was statistically significant at a 95 % confidence interval ($p < 0.05$) for all cases except for the initial rejection in experiments with water ozonated at 0.93 mg(O_3)/mg(DOC). The increase can be attributed to the changes in properties of the fouling layer, which forms in the intrapore space or on the membrane surface or both, and is capable of partially rejecting DOC. In a recent study, we showed that ozonation makes NOM-NOM interactions less favorable due to an increase in NOM polarity; the measured water contact angles on the surface of membranes fouled by Suwannee River NOM solutions decreased, as a result of

ozonation, from $(40\pm1.5)^0$ to $(30\pm1.8)^0$ at pH 8 and 1mM Ca^{2+} [34]. Given that NOM makes up most of the DOC content of surface waters such as the Lake Lansing water used in this work, the increase in DOC rejection is likely due to a higher polarity of ozonated NOM that forms the DOC-rejecting fouling layer.

DOC rejection at the final stages of filtration was lower than at the initial stages of filtration for all tested ozone dosages. This could be due to the exhaustion of the adsorption capacity of the membrane. The above interpretation of trends in DOC rejection by UF membranes is consistent with the observed increase in R_f /DOC values (Fig. 3b) and with the results of the application of the combined pore blockage-cake filtration model (Fig. 4b). Although, based on UF flux data, it was not possible to extract the value of α, the negative slope of the $\frac{d^2t}{dV^2}\left(\frac{dt}{dV}\right)$ curve indicated that pore blocking was taking place.

In NF experiments, DOC rejection (Fig. 5b) was markedly higher than rejection by UF membranes. Size exclusion was most likely the mechanism responsible for this difference although adsorption and hydrophobic interactions could have also played a role. For NF membranes, a statistically significant decrease in rejection was observed only with the feed water ozonated at 0.93 mg(O_3)/mg(DOC) (Fig. 5b).

4. Conclusions

The study focused on the effect of pre-ozonation at low ozone dosages (<1 mg(O_3)/mg(DOC)) on the permeate flux and DOC rejection performance of UF and NF membranes treating surface waters . In *nanofiltration* experiments, the DOC rejection was consistently above 92 % regardless of the ozone dosage. The fouling resistance normalized by feed DOC (i.e. fouling propensity of the feed water) was shown to decrease with an increase in ozone dosage while DOC rejection remained essentially the same. In *ultrafiltration* experiments, the DOC rejection was markedly lower (11 % to 26 %) and was found to increase slightly with an increase in the ozone dosage. The increase in rejection with the ozone dosage was interpreted to stem from the higher polarity of ozonated NOM constituting the DOC-rejecting fouling layer. The propensity of the feed water to foul UF membranes increased with the ozone dosage but the increase was statistically significant only at 82% confidence interval.

Despite a decrease in the feed DOC (from 11.7 mg/L to 10.9 mg/L) caused by ozonation, there were no statistically significant changes in the molecular weight distribution of feed organics. Therefore changes in the chemistry, not size of the foulants were responsible for the observed changes in flux and rejection by UF and NF membranes. The combined pore blockage-cake filtration model was applied to interpret NF flux data in terms of the dominant fouling mechanisms. It was shown that a) ozonated DOC has lesser propensity to enter and block same NF pores, and b) the resistance of each individual layer of organics on the NF membrane surface is lower when organics are ozonated but that the layers pack into cakes with higher specific hydraulic resistance. Despite the higher specific resistance of the cake, the overall added resistance due to fouling was lower in experiments with ozonated water.

Acknowledgements

This work was supported in part by the National Science Foundation under research grant OISE-0530174. We thank Dow-FilmTec for providing membrane samples. SJB acknowledges the support by the Korean Research Foundation Grant, funded by the Korean Government (MOEHRD) (KRF-2006-352-D00123). Dr. Susan Masten is acknowledged for providing equipment for the ozonation of the water samples. We also thank Ms. Aubrey Huynh and Dr. Jeonghwan Kim for their contributions during early stages of the project and for useful discussions.

List of Symbols

A - surface area of the membrane (m^2)

C_b - Dissolved organic carbon concentration in the bulk of the feed solution

C_0 - initial aqueous concentration of ozone ($mg \cdot L^{-1}$)

C_t - aqueous concentration of ozone at time t ($mg \cdot L^{-1}$)

C_{in} - inlet gas-phase concentration of ozone ($mg \cdot L^{-1}$)

C_{out} - outlet gas-phase concentration of ozone ($mg \cdot L^{-1}$)

C_{feed} - DOC concentration in the feed ($mg \cdot L^{-1}$)

C_{per} - DOC concentration in the permeate ($mg \cdot L^{-1}$)

f' - DOC fraction that contributes to cake growth

$k_L a_{O_3}$ - mass transfer rate of ozone (s^{-1})

J - permeate flux ($L \cdot m^{-2} \cdot h^{-1}$)

J_0 - initial permeate flux ($L \cdot m^{-2} \cdot h^{-1}$)

μ - viscosity of water ($kg \cdot m^{-1} \cdot s^{-1}$)

ΔP - transmembrane pressure differential (Pa)

R' - specific resistance of the cake ($m \cdot kg^{-1}$);

R_{c0} - initial resistance of the cake (m^{-1})

R_m - hydraulic resistance of clean membrane (m^{-1})

R_f - total added hydraulic resistance due to fouling (m^{-1})

R_{obs} - observed rejection (%)

α - pore blockage parameter ($m^2 \cdot kg^{-1}$)

δ - thickness of the cake (m)

List of Figures

List of Tables

References

1. Chellam, S., R.R. Sharma, G.R. Shetty, and Y. Wei, *Nanofiltration of pretreated Lake Houston water: Disinfection by-product speciation, relationships, and control.* Sep. Purif. Technol., 2008. **64**(2): p. 160-169.
2. Bellona, C., J.E. Drewes, P. Xu, and G. Amy, *Factors affecting the rejection of organic solutes during NF/RO treatment - a literature review.* Water Res., 2004. **38**(12): p. 2795-2809.
3. Uyak, V., I. Koyuncu, I. Oktem, M. Cakmakci, and I. Toroz, *Removal of trihalomethanes from drinking water by nanofiltration membranes.* J. Hazard. Mater., 2008. **152**(2): p. 789-794.
4. Matsui, Y., A. Yuasa, and K. Ariga, *Removal of a synthetic organic chemical by PAC-UF system I: Theory and modeling.* Water Res., 2001. **35**(2): p. 455-463.
5. Tomaszewska, M.M.S., *Removal of organic matter from water by PAC/UF system.* Water Res., 2002. **36**: p. 4137-4143.
6. Chen, D., L.K. Weavers, H.W. Walker, and J.J. Lenhart, *Ultrasonic control of ceramic membrane fouling caused by natural organic matter and silica particles.* J. Membr. Sci., 2006. **276**: p. 135-144.
7. Schlichter, B., V. Mavrov, and H. Chmiel, *Study of a hybrid process combining ozonation and microfiltration/ultrafiltration for drinking water production from surface water.* Desalination, 2004. **168**(1-3): p. 168 (1-3) 307-317.
8. Karnik, B.S., S.H. Davies, M.J. Baumann, and S.J. Masten, *The effects of combined ozonation and filtration on disinfection by-product formation.* Water Res., 2005. **39**(13): p. 2839-2850.
9. Ventresque, C., V. Gisclon, G. Bablon, and G. Chagneau, *An outstanding feat of modern technology: the Mery-sur-Oise Nanofiltration Treatment Plant (340,000 m(3)/d).* Desalination, 2000. **131**(1-3): p. 1-16.
10. Cyna, B., G. Chagneau, G. Bablon, and N. Tanghe, *Two years of nanofiltration at the Mery-sur-Oise plant, France.* Desalination, 2002. **147**(1-3): p. 69-75.
11. Crozes, G., C. Anselme, and J. Mallevialle, *Effect of adsorption of organic matter on fouling of ultrafiltration membrane.* J. Membr. Sci., 1993. **84**: p. 61-77.
12. Park, N., S. Lee, S.R. Yoon, Y.H. Kim, and J. Cho, *Foulants analyses for NF membranes with different feed waters: coagulation/sedimentation and sand filtration treated waters.* Desalination, 2007. **202**(1-3): p. 231-238.
13. Kim, H.A., J.H. Choi, and S. Takizawa, *Comparison of initial filtration resistance by pretreatment processes in the nanofiltration for drinking water treatment.* Sep. Purif. Technol., 2007. **56**(3): p. 354-362.
14. Lee, S. and C.H. Lee, *Effect of membrane properties and pretreatment on flux and NOM rejection in surface water nanotiltration.* Sep. Purif. Technol., 2007. **56**(1): p. 1-8.
15. Tarabara, V.V., F. Pierrisnard, C. Parron, J.Y. Bottero, and M.R. Wiesner, *Morphology of deposits formed from chemically heterogeneous suspensions: Application to membrane filtration.* J. Colloid Interf. Sci., 2002. **256**(2): p. 367-377.
16. Plottu, A., N. Her, B. Houssais, G. Amy, D. Gatel, and J. Cavard, *Effect of ozonated water on membrane fouling.* Water Sci. Technol: Water Supply, 2003. **3**(5/6): p. 191-197.
17. Her, N., G. Amy, A. Plottu-Pecheux, and Y. Yoon, *Identification of nanofiltration membrane foulants.* Water Res., 2007. **41**: p. 3936 - 3947.
18. Bose, P., B.K. Bezbarua, and D.A. Reckhow, *Effect of ozonation on some physical and chemical properties of aquatic natural organic matter.* Ozone Sci. Eng., 1994. **16**(2): p. 89-112.

19. Chandrakanth, M.S. and G.L. Amy, *Effects of ozone on the colloidal stability and aggregation of particles coated with natural organic matter.* Environ. Sci. Technol., 1996. **30**(2): p. 431-443.
20. Hoigne, J. and H. Bader, *Ozonation of water - Selectivity and rate of oxidation of solutes.* Ozone Sci. Eng., 1979. **1**(1): p. 73-85.
21. von Gunten, U., *Ozonation of drinking water: Part I. Oxidation kinetics and product formation.* Water Res., 2003. **37**(7): p. 1443-1467.
22. Amy, G.L., C.J. Kuo, and R.A. Sierka, *Ozonation of humic substances: Effects on molecular weight distributions of organic carbon and trihalomethane formation potential.* Ozone Sci. Eng., 1988. **10**(1): p. 39-54.
23. Chiang, P.C., E.E. Chang, and C.H. Liang, *NOM characteristics and treatabilities of ozonation processes.* Chemosphere, 2002. **46**(6): p. 929-936.
24. Yan, M., D. Wang, B. Shi, M. Wang, and Y. Yan, *Effect of pre-ozonation on optimized coagulation of a typical North China source water.* Chemosphere, 2007. **69**(11): p. 1695-1702.
25. Edwards, M. and M.M. Benjamin, *Effect of preozonation on coagulant-NOM interactions.* AWWA Journal, 1992. **84**(8): p. 63-72.
26. Jones, K.L. and C.R. O'Melia, *Ultrafiltration of proteins and humic substances: Effect of solution chemistry on fouling and flux decline. .* J. Membr. Sci., 2001. **193**: p. 163-173.
27. Tang, C.Y., Y. Kwon, and J.O. Leckie, *Fouling of reverse osmosis and nanofiltration membranes by humic acid: Effects of solution composition and hydrodynamic conditions.* J. Membr. Sci., 2007. **290**: p. 86-94.
28. Gottschalk, G., J.A. Libra, and A. Saupe, *Ozonation of water and waste water. A practical guide to understanding ozone and its application.* 2000, Weinheim, Germany: Willey-VCH.
29. Karnik, B.S., S.H.R. Davies, K.C. Chen, D.R. Jaglowski, M.J. Baumann, and S.J. Masten, *Effects of ozonation on the permeate flux of nanocrystalline ceramic membranes.* Water Res., 2005. **39**(4): p. 728-734.
30. Glaze, W.H., *Reaction products of ozone - A review.* Environ. Health Persp., 1986. **69**: p. 151-157.
31. Bader, H. and J. Hoigné, *Determination of ozone in water by the indigo method.* Water Res., 1981. **15**(44): p. 449-456.
32. Mellema, J., *The use of apparent molecular weight distribution to evaluate the transformation of natural organic matter during ozonation and biological treatment*, in *Department of Civil and Environmental Engineering*. 1998, Michigan State University: East Lansing, MI.
33. Kerc, A., M. Bekbolet, and A.M. Saatci, *Effect of partial oxidation by ozonation on the photocatalytic degradation of humic acids.* Int J of Photoenergy, 2003. **5**: p. 75-80.
34. Kim, J., W. Shan, S.H.R. Davies, M.J. Baumann, S.J. Masten, and V.V. Tarabara, *Interactions of aqueous NOM with nanoscale TiO2: Implications for ceramic membrane filtration-ozonation hybrid process.* Environ. Sci. Technol., 2009. **43**(14): p. 5488-5494.
35. Hermans, P.H. and H.L. Bredée, *Principles of the mathematical treatment of constant-pressure filtration.* J. Soc. Chem. Ind., 1936. **55T**: p. 1-4.
36. Gonsalves, V.E., *A critical investigation on the viscose filtration process.* Rec. Trav. Chim. des Pays-Bas, 1950. **69**: p. 873.
37. Hermia, J., *Constant pressure blocking filtration laws - application to power-law non-Newtonian fluids.* Trans. Inst. Chem. Eng., 1982. **60**: p. 183 -187.
38. Bowen, W.R., J.I. Calvo, and A. Hernandez, *Steps of membrane blocking in flux decline during protein microfiltration.* J. Membr. Sci., 1995. **101**(1-2): p. 153-165.
39. Iritani, E., Y. Mukai, Y. Tanaka, and T. Murase, *Flux decline behavior in dead-end microfiltration of protein solutions.* J. Membr. Sci., 1995. **103**(1-2): p. 181-191.

40. Yuan, W., A. Kocic, and A.L. Zydney, *Analysis of humic acid fouling during microfiltration using a pore blockage-cake filtration model.* J. Membr. Sci., 2002. **198**(1): p. 51-62.
41. Ho, C.C. and A.L. Zydney, *A combined pore blockage and cake filtration model for protein fouling during microfiltration.* J. Colloid Interface Sci., 2000. **232**(2): p. 389.
42. Duclos-Orsello, C., W. Li, and C.C. Ho, *A three mechanism model to describe fouling of microfiltration membranes.* J. Membr. Sci., 2006. **280**(1-2): p. 856.
43. Tracey, E.M. and R.H. Davis, *Protein fouling of track-etched polycarbonate microfiltration membranes.* J. Colloid Interface Sci., 1994. **167**(1): p. 104-116.
44. Ho, C.C. and A.L. Zydney, *A combined pore blockage and cake filtration model for protein fouling during microfiltration.* J. Colloid Interface Sci., 2000. **232**(2): p. 389-399.
45. Rosario-Ortiz, F.L., S.A. Snyder, and I.H.M. Suffet, *Characterization of disolved organic matter in drinking water sources impacted by multiple tributaries.* Water Res., 2007. **41**(18): p. 4115-4128.
46. Hyung, H., S. Lee, J. Yoon, and C.H. Lee, *Effect of preozonation on flux and water quality in ozonation-ultrafiltration hybrid system for water treatment.* Ozone Sci. Eng., 2000. **22**(6): p. 637-652.
47. Wang, X.D., L. Wang, Y. Liu, and W.S. Duan, *Ozonation pretreatment for ultrafiltration of the secondary effluent.* J. Membr. Sci., 2007. **287**(2): p. 187-191.

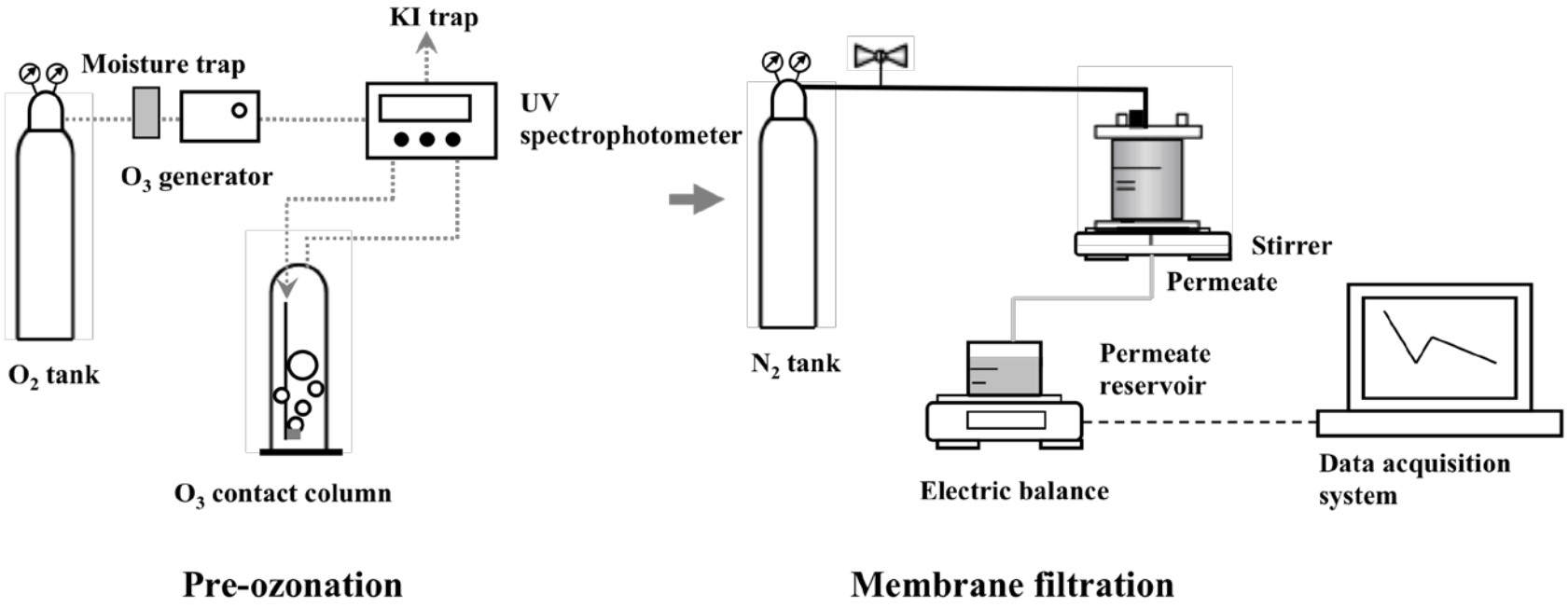

Figure 1: Schematic of the experimental apparatus

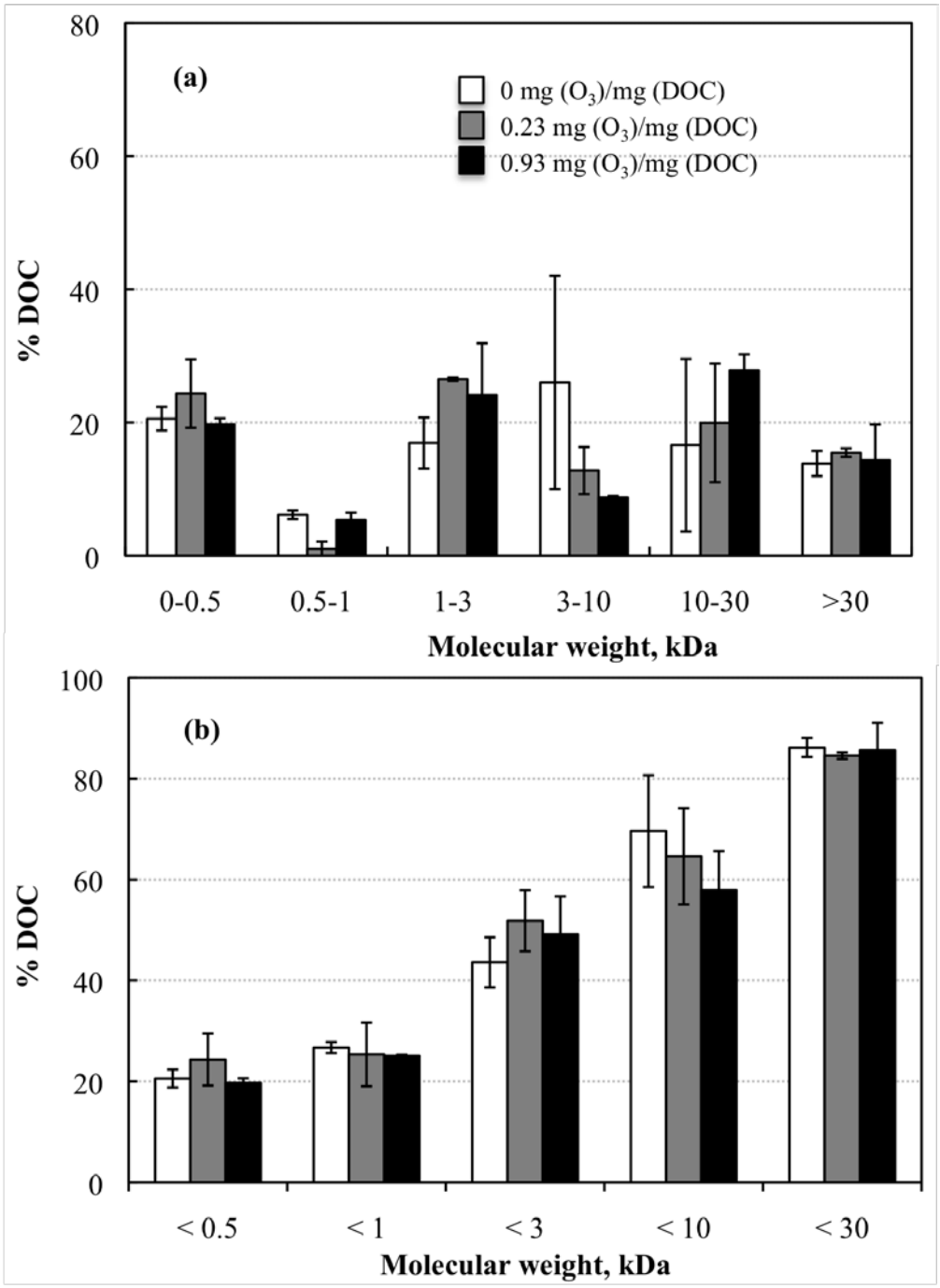

Figure 2: Differential (a) and accumulative (b) molecular weight distribution of DOC in ozonated Lake Lansing water as a function of ozone dosage

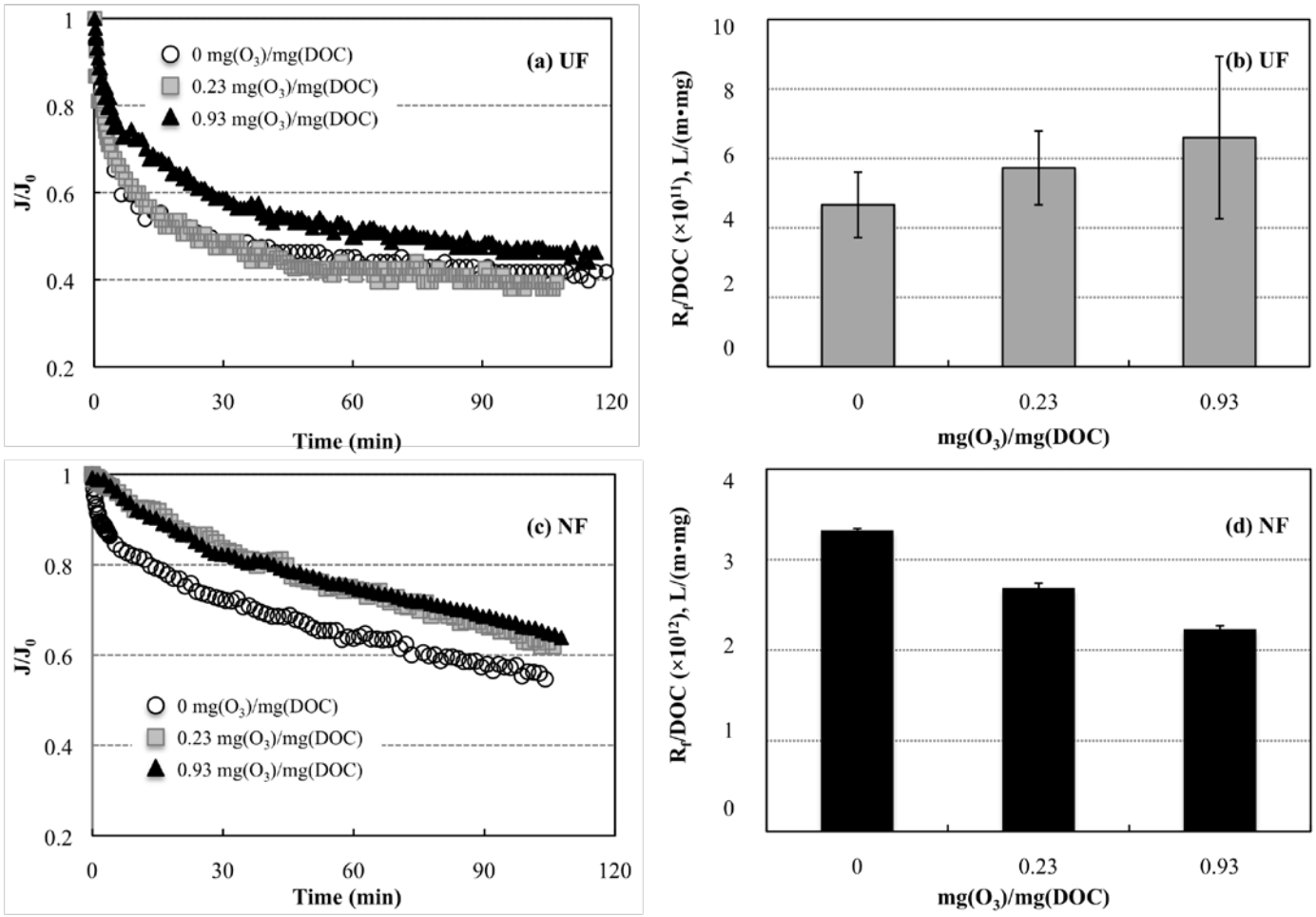

Figure 3: Normalized permeate flux (a, c) and fouling propensity of feed water (expressed as added hydraulic resistance normalized by the feed DOC) (b, d) as functions of applied ozone dosage in ultrafiltration (a, b) and nanofiltration (c, d) experiments. Error bars in Figures 3b and 3d correspond to 95 % confidence intervals.

Note: The initial permeate flux, J_0, was 0.45 ± 0.07, 0.40 ± 0.10, 0.32 ± 0.13 mL/min/cm^2 at 0, 0.23, 0.93 mg(O_3)/mg(DOC) for UF membrane and 0.12 ± 0.0, 0.12 ± 0.0, 0.13 ± 0.0 mL/min/cm^2 at 0, 0.23, 0.93 mg(O_3)/mg(DOC) for NF membranes

(a)

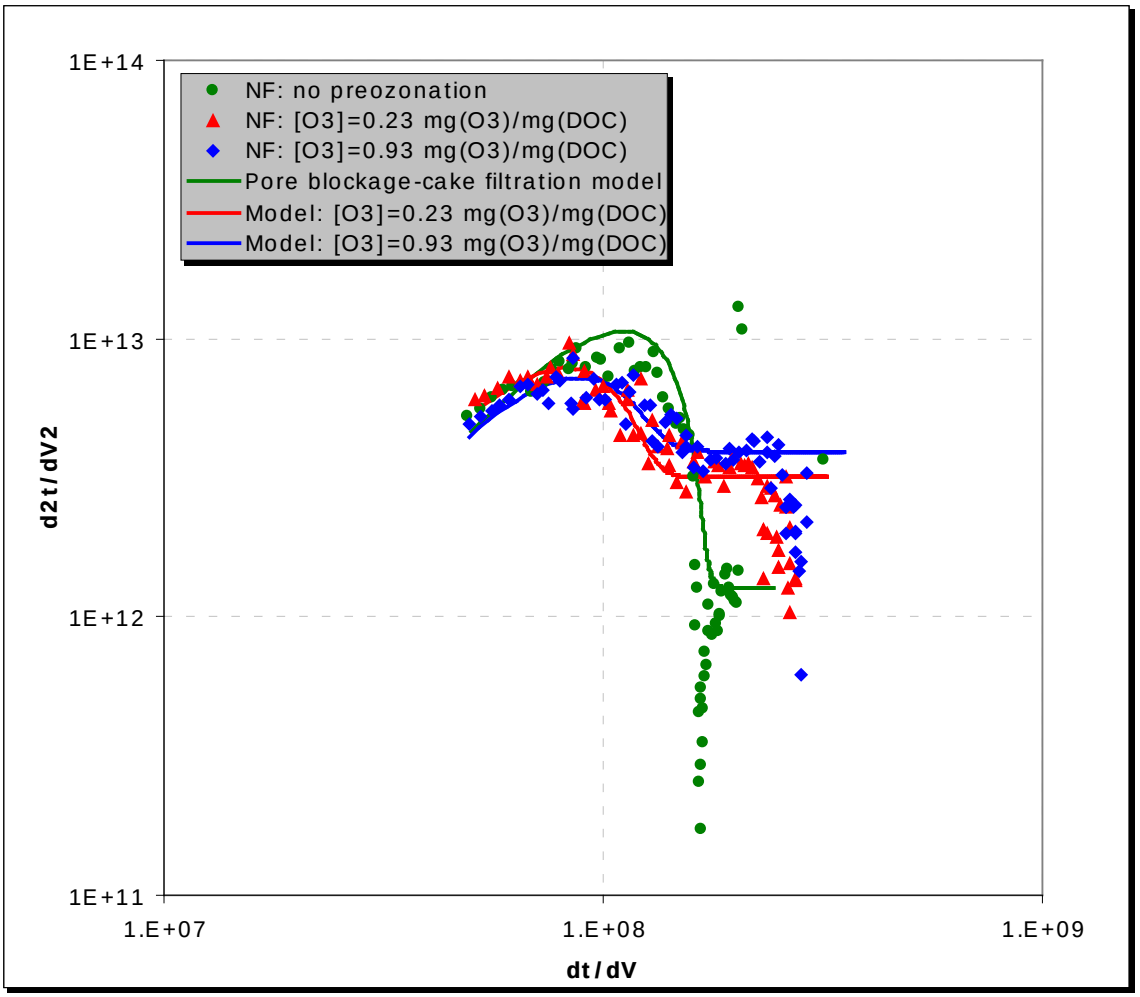

Figure 4: Flux decline analysis for the filtration of ozonated surface water by NF (a, b) and UF (b) membranes. Experimental data are from Fig. 3 (a, c)

1
2

1

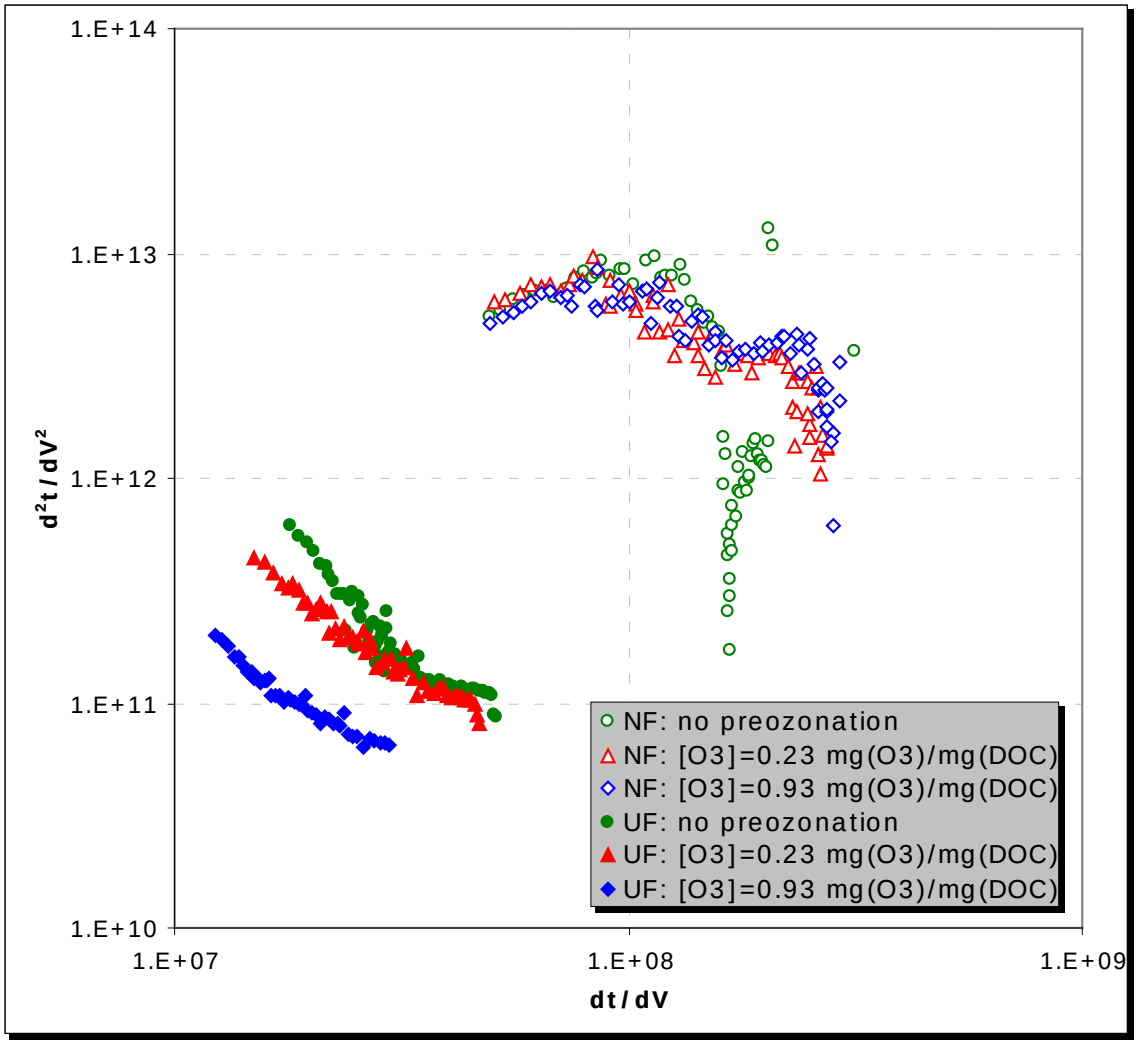

Figure 4 (continued)

2
3

1

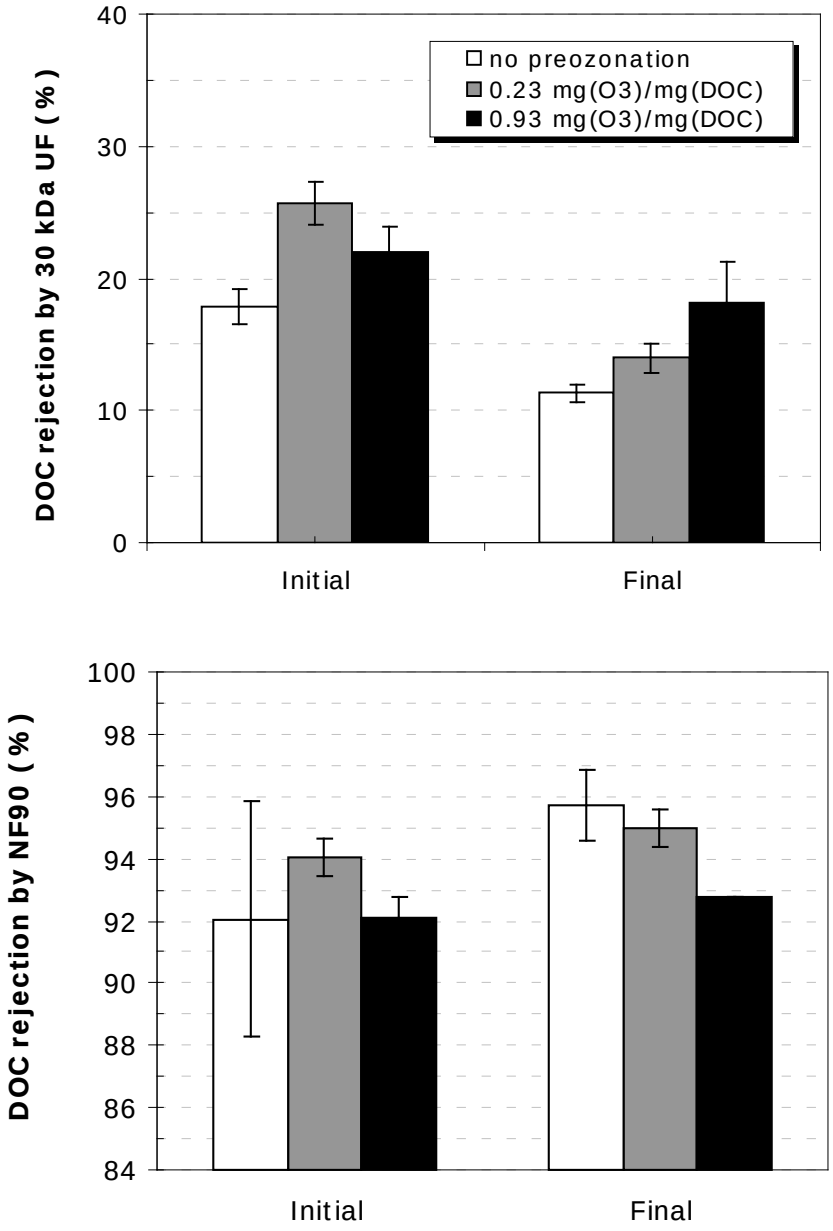

Figure 5: DOC rejection by UF and NF membranes as a function of ozone dosage. The error bars correspond to a 95 % confidence interval.

2

1

Ozone dosage,	pH	Conductivity,	DOC,	Abs_{436}	UV_{254},	SUVA*,	Zeta potential,
$mg(O_3)/mg(DOC)$		$\mu S \cdot cm^{-1}$	mg/L	cm^{-1}	1/cm	L/mg/cm	mV
0#	8.01	351	11.7 ± 0.04	0. 013	0.223	2.03	-17.4 ± 0.9
0.23	8.15	349	11.6 ± 0.01	0.009	0.164	1.50	-17.6 ± 0.5
0.93	8.28	345	10.9 ± 0.10	0.008	0.112	1.03	-15.2 ± 0.7

2

Table 1: Physicochemical properties of Lake Lansing water, pre-filtered through a 0.5 μm filter, as a function of applied ozone dosage.

* Specific UV absorbance (L/mg·cm) = $UV_{254}/DOC \times 100$

\# The raw water had the following characteristics [8, 29]: calcium concentration 0.2 mg/L; alkalinity 150 mg/L as $CaCO_3$; total phosphate 0.06 mg/L; and hardness (190 to 198) mg/L as $CaCO_3$.

3
4

Parameter	UF	NF
Membrane	YMJWSP3001	NF90
Membrane material	polyvinylidene fluoride	aromatic polyamide
MWCO, Da	30,000	200 to 400
Contact angle	$85^{o} \pm 3^{o}$	$66^{o} \pm 2^{o}$
Streaming potential, mV	-13.0 ± 1.0	-5.5 ± 0.5

Table 2: Properties of membranes

Membrane type	Ozone dosage, $[O_3]/C_b$ (mg/mg)	Membrane resistance, R_m (m^{-1})	Transmembrane pressure, ΔP (MPa)	DOC feed concentration, $C_{DOC}\cdot10^{-3}$ (kg/m^3)	Initial flux, $J_0\cdot10^{-5}$ (m/s)	Pore blockage parameter, α (m^2/kg)	Initial cake resistance, R_{c0} (m^{-1})	Cake growth parameter, $f'\cdot R'$ (m/kg)
NF90	0	$44.7\cdot10^{12}$	1.000	11.7	1.853	$0.92\cdot10^{4}$	$14.6\cdot10^{13}$	$0.32\cdot10^{17}$
	0.23	$44.0\cdot10^{12}$	1.000	11.6	1.831	$1.58\cdot10^{4}$	$6.6\cdot10^{13}$	$3.78\cdot10^{17}$
	0.93	$44.0\cdot10^{12}$	0.828	10.9	1.864	$1.82\cdot10^{4}$	$5.7\cdot10^{13}$	$6.24\cdot10^{17}$
UF PVFD 30kDa	0	$6.3\cdot10^{12}$	0.345	11.7	4.1	Poor quality of the fit by the combined pore blockage-cake filtration model		
	0.23	$5.1\cdot10^{12}$	0.310	11.6	7.2			
	0.93	$2.8\cdot10^{12}$	0.221	10.9	11.0			
MF 0.2 μm track etched [41]	0	$3.8\cdot10^{6}$	0.035	0.25; 1; 2; 4	92.5	4.9	$1.3\cdot10^{11}$	$5.7\cdot10^{13}$

Table 3: Experimental variables and best fit values of the combined pore blockage-cake filtration model parameters